

# AFRRI's Gamma-Ray, X-Ray, and Fission-Neutron Calibration Curves for the Lymphocyte Dicentric Assay: Application of a Metaphase Finder System

P.G.S. Prasanna<sup>1</sup>

H. Loats<sup>2</sup>

H.M. Gerstenberg<sup>1</sup>

B.N. Torres<sup>1</sup>

C.W. Shehata<sup>1</sup>

K.L. Duffy<sup>1</sup>

R.S. Floura<sup>1</sup>

A.W. Khusen<sup>1,3</sup>

W.E. Jackson<sup>1</sup>

W.F. Blakely<sup>1</sup>

<sup>1</sup>Armed Forces Radiobiology Research Institute, Applied Cellular Radiobiology and Radiation Sciences Departments, 8901 Wisconsin Avenue, Bethesda, MD 20889-5603

<sup>2</sup>Loats Associates Inc., 201 East Main Street, Westminster, MD 21157

<sup>3</sup>Current address: Center for Standardization and Radiological Safety Research, National Atomic Energy Agency, Jakarta, Indonesia

Armed Forces Radiobiology Research Institute

8901 Wisconsin Avenue  
Bethesda, Maryland 20889-5603  
[www.afri.usuhs.mil](http://www.afri.usuhs.mil)

Cleared for public release; distribution unlimited.

AFRRI Special Publication 02-1

Printed May 2002

---

This and other AFRRI publications are available to qualified users from the Defense Technical Information Center, Attention: OCP, 8725 John J. Kingman Road, Suite 0944, Fort Belvoir, VA 22060-6218; telephone (703) 767-8274. Others may contact the National Technical Information Service, 5285 Port Royal Road, Springfield, VA 22161; telephone (703) 487-4650.

## Contents

---

Foreword . . . . .	v
Précis . . . . .	vi
Introduction . . . . .	1
Materials and Methods . . . . .	3
Results and Discussion . . . . .	7
Appendix . . . . .	13
References . . . . .	15



## Foreword

---

Established in 1961, the Armed Forces Radiobiology Research Institute (AFRRI) is the sole Department of Defense research laboratory for medical radiological defense. Its primary mission is to develop medical countermeasures against ionizing radiation. Developmental and applied research focuses on prevention, assessment, and treatment of radiological injury, and on the confounding problems of combined injury involving radiation and other battlefield stressors.

Precision and accuracy are hallmarks of effective and meaningful biological tests. This is especially true for the lymphocyte-dicentric assay as it applies to biological dosimetry and to the estimation of radiation doses in individuals. Gamma rays, x rays, and fission neutrons induce morphologic aberrations in lymphocyte chromosomes that can be quantifiably measured using sophisticated cytogenetic techniques. The dicentric chromosome is one such aberration, and it is recognized as a biomarker of exposures to ionizing radiation. Measuring the frequency of dicentric chromosomes in peripheral blood lymphocytes gives a good approximation of radiation dose. Accordingly, the lymphocyte dicentric assay finds utility in cases of accidental or intentional exposures when there is a need to document radiation doses in individuals, and the assay's predictive value (precision and accuracy) is of paramount importance when used to aide medical triage and manage the radiation injured.

The lymphocyte-dicentric assay is a technically demanding and time-consuming procedure, requiring a highly trained technical or professional staff. Even with highly qualified individuals, controlling inter-laboratory variability is problematic. Each laboratory must therefore develop

and periodically update its own calibration curves in order to achieve an acceptable performance standard. Predictive value is enhanced further when each radiation type for which a calibration curve is generated is fully characterized relative to microdosimetric parameters. These high standards are employed by the AFRRI Biological Dosimetry Team and are described in this report.

A major research thrust of the team is to improve the performance characteristics of cytogenetic tests. Through a collaborative effort under a cooperative research and development agreement with Loats Associates Inc., Westminster, Maryland, the team has developed an enhanced digital-image and neural network system for automated image analysis. Data collection for this report was facilitated using the system's mature automated metaphase-finding component coupled with lymphocyte-dicentric scoring at peripheral, or satellite, scoring stations.

In addition to its core objective of developing, testing, and validating deployable biodosimetry systems for military field operations, the team maintains one of the nation's few reference testing facilities for radiation dose assessment. This resource responds to military, domestic, and international nuclear or radiological emergencies involving human exposures to ionizing radiation. It is for this reason that the studies reviewed in this report were undertaken.

The accomplishments documented herein point to the critical role of radiobiological research in defending our nation against current and future threats through medical readiness, on both military and Homeland Security fronts.

ROBERT R. ENG, COL, MS, USA  
DIRECTOR, ARMED FORCES RADIOBIOLOGY  
RESEARCH INSTITUTE

## Précis

---

Facilities are established at the Armed Forces Radiobiology Research Institute (AFRRI) to perform radiation-induced chromosome aberration analysis for biological dosimetry. Whole blood from healthy human volunteers was used after obtaining informed consent. Peripheral blood lymphocytes were exposed *in vitro* to different types of radiation;  $^{60}\text{Co}$  gamma rays ( $\bar{E}_\gamma=1.25$  MeV, mean of the absorbed dose distribution of the lineal energy,  $\bar{y}_D=1.9$  keV/ $\mu\text{m}$ , 1 Gy/min); x rays (250 kVp,  $\bar{E}=83$  keV,  $\bar{y}_D=4$  keV/ $\mu\text{m}$ , 1 Gy/min); or a fission-spectrum neutron source ( $\bar{E}=0.71$  MeV,  $\bar{y}_D=65$  keV/ $\mu\text{m}$ , 0.25 Gy/min). Distribution of radiation-induced dicentrics among cells exhibited Poisson statistics as characterized by the Papworth method (Papworth 1970). Dose-response relationships for the yield of dicentrics for photon sources were fitted with a linear-quad-

ratic model using the maximum-likelihood method for the neutron source by a weighted linear regression method.

Comparison of the data with other published studies is presented. The dose-response relationships for dicentric induction by low- and high-linear energy transfer (LET) radiation are consistent with the single- and two-track model of aberration formation,  $Y = \alpha D + \beta D^2$ . An increase in  $\bar{y}_D$  resulted in an increase in dicentric yield. As expected, fission neutrons induced a significantly higher yield of dicentrics than that caused by low-LET sources. The linear component of the model, corresponding to damage caused by single-tracks, is predominant with fission neutrons so that the dose-effect relationship is essentially linear. An automated metaphase finder system with a satellite scoring utility was used to improve data collection.

## Introduction

---

Application of the lymphocyte-dicentric assay for biological dosimetry has made significant contributions in both accidental and occupational overexposures. This biological dosimeter is the most thoroughly investigated system (Muller and Streffer 1991). Dicentrics are considered relatively radiation specific; only a few chemicals are known to interfere with this assay. Low background levels (about 1 dicentric in 2000 cells), high sensitivity (a threshold dose of 0.05 Gy), and known dose dependency up to 4 Gy (for low-LET radiation) make this assay quite robust (Greenstock and Trivedi 1994). Effects of radiation quality and dose rate are well characterized (Edwards 1997). The influence of time between radiation exposure and analysis for a broad dose range is not critical for at least the first 2 weeks after exposure (I.A.E.A. 2001). However, published reports show that differences exist in the measured yield of dicentrics per Gy among several laboratories (Lloyd *et al.* 1987). Therefore, it is advised that each laboratory should establish its own calibration curves for the induction of dicentrics by different radiation types over a range of doses and dose rates (I.A.E.A. 2001).

Dicentric yield from radiation exposure is dependent not only on the dose, but also on radiation quality. Radiation quality depends on microscopic energy deposition events that are characterized by temporal, spatial, and energy distributions of the radiation fields within the irradiated volume. There is evidence that radiobiological effects are more closely related to lineal energy than to neutron energy (I.C.R.U. 1980). Furthermore, it has been stated that the

macroscopic radiation descriptors such as dose, LET, and relative biological effectiveness (RBE) are inadequate, if not irrelevant, parameters for the quantification of biological effects of ionizing radiation (Watt *et al.* 1994). A characteristic of ionizing radiation is that its energy can be dissipated in terms of discrete packets, e.g., spurs and blobs, the number and magnitude of which can be determined by microdosimetry (I.C.R.U. 1993). While the absorbed dose reflects the macroscopic deposition within a given material, it is microdosimetry, with parameters such as lineal energy  $y$  and its dose- and frequency-weighted mean values  $\bar{y}_D$  and  $\bar{y}_F$  that describes the radiation energy interactions at the microscopic level. Bauchinger reviewed the importance of microdosimetry on the classical and alternative mechanisms of chromosome-aberration formation (Bauchinger 1983).

This paper reports dose-response or calibration curves of measured dicentric yields following exposure to 250-kVp x rays,  $^{60}\text{Co}$  gamma rays, and fission neutrons, whose radiation qualities have been measured at AFRRI (Bethesda, MD) in terms of their microdosimetric parameters. In addition, we compare these dose-response calibration curves with similar studies from other laboratories. Estimating radiation dose by chromosome aberration analysis requires time-demanding and labor-intensive scoring by expert cytogeneticists. Our attempt to decrease cytogenetic scoring time in biodosimetric assessment for radiation accidents is addressed by the use of satellite scoring stations used in conjunction with an automated metaphase finder.

## Dose Response Relationships for Dicentric Yield

## Materials and Methods

**Lymphocytes.** Whole blood from healthy human donors was collected into vacutainers containing ethylenediamine tetraacetic acid (EDTA) (Becton-Dickinson, Rutherford, NJ). The informed consent form used in this study was approved by the Uniformed Services University of the Health Sciences, Human Use Committee (Bethesda, MD). Lymphocytes were isolated using a density gradient (Histopaque 1077, Sigma Chemical Co., St. Louis, MO), washed with phosphate buffered saline (PBS), and resuspended in complete growth medium (Karyomax, bone marrow karyotyping medium, Life Technologies, Rockville, MD) at a concentration  $1\text{-}1.5 \times 10^6/\text{ml}$  for exposure to different radiation types.

**Radiation sources and dosimetry.** Dosimetry procedures and radiation sources used in these studies were previously described for  $\gamma$  rays (Stankus *et al.* 1995; Prasanna *et al.* 1998), x rays (Redpath *et al.* 1995; Blakely *et al.* 1995; Prasanna *et al.* 1997), and fission neutrons (Redpath *et al.* 1995; Blakely *et al.* 1995; Prasanna *et al.* 1997). Measured lineal energy dose distributions for AFRRI's gamma rays, x rays, and fission neutrons are shown in Figure 1.

Gamma-ray exposures were performed in the bilateral field of the  $^{60}\text{Co}$  facility at AFRRI as described earlier (Carter and Verrelli 1973). The dose rate was measured with a tissue-equivalent ionization chamber before irradiation following a well-established dosimetry protocol (A.A.P.M. 1983). The field was uniform within 2%. Cells in suspension were placed in 15-ml polypropylene centrifuge tubes and irradiated at room temperature at a dose rate of 1 Gy/min. The  $\bar{y}_F$  where  $\bar{y}_F = \text{LET}_\infty$  (Turner 1992; Rossi 1959), measured using a 1- $\mu\text{m}$  diameter tissue-equivalent proportional counter (TEPC), has been previously described (Stankus *et al.* 1995). X-ray irradiation was performed using a 320-kVp Philips industrial x-ray machine (GMBH, Hamburg, Germany), with an effective energy of

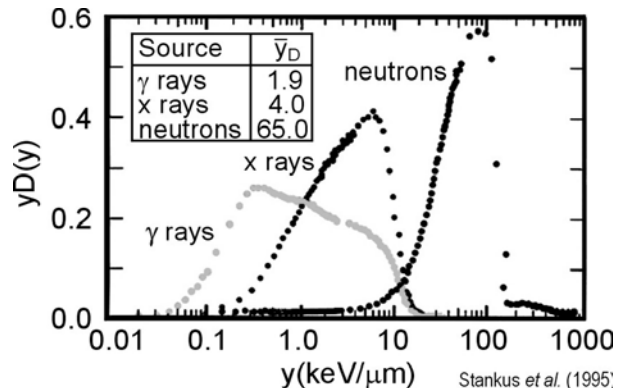


**Figure 1.** Measured lineal-energy dose distributions for AFRRI's gamma rays, x rays, and fission neutrons. The measurements were made using a TEPC detector with a gas filling made using a pressure corresponding to a 1- $\mu\text{m}$  diameter. The dose distributions,  $d(y)$ , are normalized to unit dose and plotted as  $y \cdot d(y)$ . In a semi-logarithmic representation such as this, the area under a curve delimited by any two values of  $y$  proportional to the fraction of dose delivered by events with lineal energies in this range. This is the standard representation of microdosimetric spectra. The region of the gamma-ray spectrum below  $0.1 \text{ keV } \mu\text{m}^{-1}$  is explained in Stankus *et al.* (1995). The definitions and references for the published data are in the text. However, these distributions may vary depending on experimental arrangements and measurement parameters.

83 keV (source to sample distance = 55.2 cm, 250 kVp at 12.5 mA, 0.2-mm Cu and 1-mm Al filtration) at doses between 0.5 and 3.5 Gy. Dosimetry was performed using ion chambers placed in tissue-culture flasks filled with tissue-equivalent plastic as described by the International Commission on Radiation Units and Measurements (ICRU) (I.C.R.U. 1973). Field uniformity was within 2%. Cells in suspension in 25- $\text{cm}^2$  tissue-culture flasks were placed on a rotating Plexiglas holder for irradiation and exposed at room temperature at a dose rate of 1 Gy/min. The  $\bar{y}_F$  for this x-ray source has been previously described (Blakely, Benevides and Gerstenberg 1995; Prasanna *et al.* 1997).

Neutron irradiation was performed using AFRRI's training, research, isotope, General Atomic (TRIGA) Mark-F, nuclear reactor. Samples for irradiation were placed in a lead box with 5-cm thick walls. Additional 15 cm of lead shielding was placed in front of the reactor tank wall, and borated polyethylene slabs were placed around the sides of the tank wall, which projected into the exposure room. The lead box was mounted on a wooden table and rolled along a track to allow the array to be placed at a reproducible distance from the reactor core. An extractor system was used for placing and retrieving the samples within the lead box (Redpath *et al.* 1995). Cells were suspended in 15-ml polypropylene centrifuge tubes, placed in a Plexiglas holder, and exposed at room temperature. The dose rate and neutron and gamma portions of the mixed field radiation configuration were determined using the paired-ion chamber technique (I.C.R.U. 1977) and applying previously determined spectral information for this radiation configuration (Verbinski *et al.* 1981). The dose rate was 0.25 Gy/min. The neutron to total dose ratio was  $0.95 \pm 0.07$ . Fluence-weighted mean energies ( $\bar{E}$ ) for this configuration are 0.71 MeV for neutrons (N.I.S.T. 1991) and 1.80 MeV for gamma rays (Zeman and Ferlic 1984). The radiation field was uniform to within 2.5%. The  $\bar{y}_F$  for this  $^{235}\text{U}$  reactor produced the degraded fission-neutron spectra that have been previously described (Blakely, Benevides and Gerstenberg 1995; Prasanna *et al.* 1997).

Previous studies have estimated  $\bar{y}_F$  for spherical volumes with 10- $\mu\text{m}$  diameters (the mean diameter of the human lymphocytes used in this work) for x-ray and fission neutron radiation qualities (Blakely, Benevides and Gerstenberg 1995; Prasanna *et al.* 1997). The  $^{60}\text{Co}$  gamma-ray  $\bar{y}_F$  was measured to be 0.39 keV/ $\mu\text{m}$  using a TEPC detector with gas pressure corresponding to a 1- $\mu\text{m}$  diameter. The  $\bar{y}_F$  for 10  $\mu\text{m}$ , 0.53 keV/ $\mu\text{m}$  was obtained by linear interpolation of  $^{60}\text{Co}$   $\bar{y}_F$  data (Biavati and Boer 1996) determined with a walled TEPC detector having equivalent diameters from 0.5 to 20  $\mu\text{m}$ . Biavati and Boer's measured value at 1- $\mu\text{m}$

diameter (Biavati and Boer 1996) was in excellent agreement with our value determined at the same diameter.

The number of neutron hits per cell nucleus was determined from the dose and fluence relationship as previously described (Keifer 1990) and the assumption that  $\text{LET} = \bar{y}_F$ , a mean cell diameter of 10  $\mu\text{m}$ , and the designated dose. The hit frequency was then calculated assuming a Poisson distribution of hits (Fisher and Harty 1982). Similar calculations were performed for the  $^{60}\text{Co}$  gamma-ray source using a LET value of 0.23 keV/ $\mu\text{m}$  (I.C.R.U. 1980). The same was done for the x-ray source, with the assumption that the literature value of 1.7 keV/ $\mu\text{m}$  for 200 keV x rays held for the 250 kVp x-ray source.

**Lymphocyte culture and metaphase spread preparation.** Following exposure to radiation, the lymphocytes were washed and re-suspended in media, stimulated to grow by adding phytohemagglutinin (0.5  $\mu\text{g}/\text{ml}$ ; Murex Diagnostics Ltd, Dartford, England), and incubated at 37 °C. After 44 h of stimulation, colcemid was added (1  $\mu\text{g}/\text{ml}$ ; Sigma Chemical Co., St. Louis, MO) to stop cell cycle progression in first division metaphases and then incubated for an additional 4 h. Less than 3% of the metaphases were in second division metaphases as determined by the fluorescence plus Giemsa technique at this culture time (data not shown). Following hypotonic treatment in 1% sodium-citrate solution, cells were fixed in 1:3 acetic methanol. Metaphase spreads were prepared on acid-cleaned glass slides by the standard method (Preist 1977). The slides were stained in 4% Giemsa in PBS for dicentric analysis.

**Automated metaphase-finding and dicentric analysis.** Figure 2 illustrates the automated metaphase finder system, software utilities, and satellite-scoring concept used in these studies. Slides were placed on the stage of an automated metaphase finder (LAI Metafind, Loats Associates Inc., Westminster, MD). This system

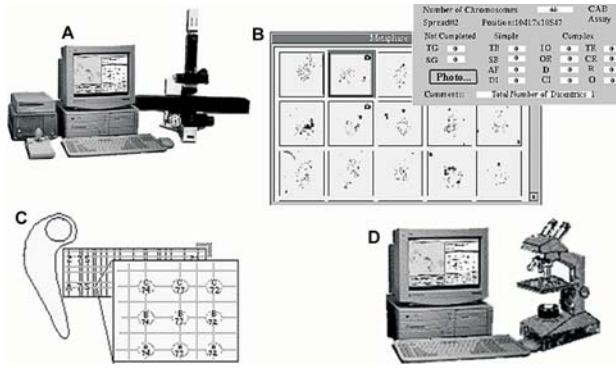


**Figure 2.** Automated metaphase-finding and analysis of aberrations in satellite-scoring stations. The automated metaphase finder (A) consists of a microscope equipped with a 16-slide capacity stage, motorized x-, y-, and z-axis computer-controlled positioning with specially adapted auto-focal capabilities. Accuracy of position in the x-, y-, and z-axes are within 0.5  $\mu\text{m}$ , 0.5  $\mu\text{m}$ , and 0.05  $\mu\text{m}$ , respectively. Images of spreads are acquired using a three-chip RGB color camera and color-digitizer board. The system automatically locates scorable metaphase spreads at low magnification, and saves image and location of each spread on a slide (B). An England finder slide (C) is used to calibrate precise location coordinates. Software utilities were developed to permit the metaphase finder system to relocate a spread for analysis either in the metaphase finder or in the satellite-scoring station (D).

consists of a standard binocular microscope (Olympus, Japan) equipped with a 16-slide capacity stage and motorized x-, y-, and z-axis computer-controlled positioning with specially adapted auto-focal capabilities. The system includes specialized software utilities (Loats Associates Inc., Westminster, MD) that permit user

control of image recognition parameters and relocation of metaphase spreads on the 16-slide capacity microscope and stand-alone microscopes, here referred to as satellite scoring stations. Images of metaphase spreads were acquired using a color camera and a color-digitizer board. Images were displayed on a computer monitor. The metaphase spreads were located using a 10-x magnification objective lens and were relocated with a 100-x magnification objective on slides by the system for manual chromosome aberration analysis. Alternatively, the slide and vernier locations of the collected spreads were transferred to satellite scoring stations, and the relocation of spreads using a 100-x magnification objective was done for manual dicentric analysis by several investigators.

**Data Analysis.** Dose-response relationships for the yield of dicentric for photon sources were fitted by the linear-quadratic model  $Y = \alpha D + \beta D^2$  using the maximum-likelihood method and for the neutron source by the weighted linear regression model  $Y = \alpha D$ . Weights were based on the reciprocal of the standard error (SE) of the mean squared. Correlation coefficients ( $r$ ) of the fitted models were also determined. The analysis of the yield of dicentric in metaphases included the determination of the mean  $\pm$ SE and the evaluation of the frequency distribution using the  $\sigma^2/y$  and  $\mu$  test of Papworth (Papworth 1970). Using the Papworth test, a  $\mu$  value between -1.96 and 1.96 indicates overdispersion.

## Dose Response Relationships for Dicentric Yield

## Results and Discussion

**Radiation quality and microdosimetry.** In contrast to the common low-LET photon sources (250-kVp x rays,  $^{60}\text{Co}$  gamma rays), the quality of high-LET neutron sources can vary considerably. Neutrons are classified according to their energies (Attix 1986). Thermal neutrons have energies less than 0.5 keV (Attix 1986). Intermediate energy neutrons, sometimes referred to as “slow,” “intermediate,” “resonance,” or “epithermal” neutrons, have energies from 0.5 keV up to 10 keV. Neutrons with energies above 10 keV but below 20 MeV are called “fast” neutrons, and those with energies above 20 MeV are called “relativistic” neutrons (Turner 1992).  $^{235}\text{U}$ -fission reactor neutrons produce energies in the range from above 0.1 keV to over 10 MeV (I.C.R.U. 1977) and hence include mostly slow and fast neutrons. Degraded fission spectrum neutrons, commonly used in radiobiology studies, are often referred to as fission spectrum neutrons.

In these studies, the dose rate for the photon sources was 1 Gy/min. A fourfold lower dose rate (25 cGy/min) was used for the fission-neutron studies. Figure 3 illustrates the typical time versus dose-rate profile from a single run. Steady state conditions were obtained after 1 min. Neutron exposure intervals spanned 1.9 to 8 min in these studies.

Radiation qualities for the sources used in this study were extensively characterized (Fig. 1). Table 1 lists the radiation dosimetric parameters for the gamma-ray, x-ray, and degraded fission-spectrum neutron sources used to irradiate human lymphocytes *in vitro*. Measured values for they  $\bar{y}_D$  were determined for 1- $\mu\text{m}$  diameter volumes and ranged from 1.9 to 65 keV/ $\mu\text{m}$ . The  $\bar{y}_F$  values are shown for 10- $\mu\text{m}$  diameter volumes and span approximately a 50-fold range (0.35 to 18 keV/ $\mu\text{m}$ ). Lymphocytes were exposed to these sources over dose ranges as shown in Table 1. Cell fractions receiving no hits were negligible (less than  $1 \times 10^{-3}$ ) at these doses, but the hit frequency per nucleus varied

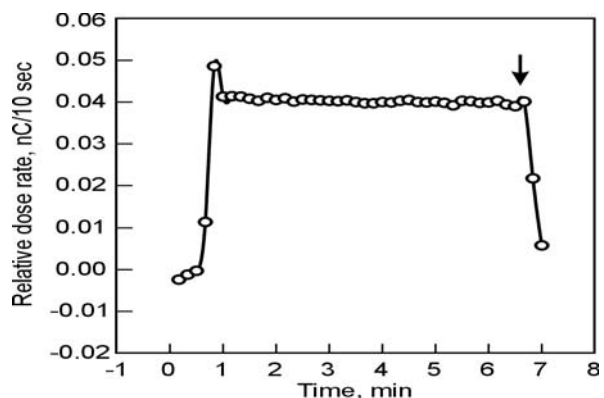


**Figure 3.** Dose-rate and time-course for neutron exposure. This figure illustrates dose and dose-rate measurements from a typical experiment where samples were exposed to fission neutrons. Each neutron run was selectively monitored using fission and ionizing chambers in the exposure room. The time course of dose measurements detected with a  $0.5 \text{ cm}^3$  ionizing chamber for a 1.5-Gy dose at  $0.25 \text{ Gy min}^{-1}$  is illustrated. Data measured in units of nC/10-sec interval are integrated for each run and analyzed to determine dose and dose rate. The sample placed in the lead box was extracted from the exposure room just before the fall in the relative dose rate after 6 min, indicated by the arrow ( $\downarrow$ ).

with relative progressive increases for neutrons, x rays, and gamma rays, 1:11:79-fold respectively (Fig. 1).

AFRRI's fission neutron facility produces a radiation quality that is qualitatively similar to other  $^{235}\text{U}$ -reactor fission-neutron facilities, including Janus located at Argonne National Laboratory (ANL, Argonne, IL) (Marshall and Williamson 1985), British Experimental Pile (BEPO) located at the National Radiological Protection Board, Harwell, UK (Lloyd *et al.* 1976; Scott *et al.* 1969), and the reactor neutron therapy converter (RENT) located in Germany (Bauchinger *et al.* 1984). There are both similarities and differences in the radiation qualities of these sources. The TRIGA and Janus microdosimetry spectra have been compared and found nearly identical (Gerstenberg 1991). In

**Table 1.** Radiation dosimetry parameters used to irradiate human lymphocytes *in vitro*.

Radiation type	$\bar{E}$ (MeV) <sup>a</sup>	$\bar{y}_F$ (keV/ $\mu$ m) <sup>b, c</sup>	$\bar{y}_D$ (keV/ $\mu$ m) <sup>d, e</sup>	Dose rate (Gy/min)	Dose range (Gy)	Mean Number Of hits/nucleus/Gy <sup>f</sup>
<sup>60</sup> Co gamma rays	1.25	0.35	1.9	1.0	0.25 - 5.0	2134
250-kVp x rays	0.083	1.53	4.0	1.0	0.25 - 3.5	289
Fission neutrons	0.71	18.0	65.0	0.25	0.75 - 2.5	27

a.  $\bar{E}$  is the mean energy.  
b.  $\bar{y}_F$  is the frequency-weighted mean of the lineal energy.  
c. Equivalent detector diameter of 10 $\mu$ m.  
d.  $\bar{y}_D$  is the dose-weighted mean of the lineal energy.  
e. Equivalent detector diameter of 1 $\mu$ m.  
f. Cell fractions receiving no hits were negligible (less than 1 x 10<sup>-3</sup>) in samples exposed to designated doses of any of these radiation sources.

contrast, the RENT source has significantly higher mean neutron energy (1.6 MeV) compared to the neutron energy (0.7 MeV) for the TRIGA or Janus sources. This difference can be attributed to the thickness of the high atomic number (Z) material that the beam transverses. RENT's neutron beam is filtered by 2.5 cm of lead, while the TRIGA neutron beam transverses 20 cm of lead. It should be noted that for a typical fission spectrum, when filtered through lead, the neutron spectrum peak would be shifted down in energy. This shift is due to the energy dependence of the inelastic neutron cross-section for lead or any high Z-material, creating neutrons below 1 MeV. These neutrons are built-up by the higher-energy neutrons scattering to a lower energy. This is consistent with Eisenhower's calculation (Eisenhower 1991) that an increase in the thickness of lead at AFRRI's reactor results in a progressive decrease in the mean neutron energy. An opposite shift occurs in the lineal-energy spectrum where calculations show that the peak moves up in lineal energy; the resulting spectrum peak will be shifted up in y value from 50 to almost 90 keV/ $\mu$ m when no lead is present compared with 20 cm of filtered lead (Gerstenberg 1989). The mean value of the spectrum  $\bar{y}_D$  also shifts, but not so dramatically because of the change in the shape of the y spectra.

**Automated metaphase-finding.** Several thousand metaphases from numerous healthy donors were analyzed to establish radiation-calibration curves for the induction of dicentric formation. Collection of this data from slides was

efficiently and rapidly accomplished by the use of an automated metaphase finder. The metaphase spreads were either automatically re-located by the system or the digital data on location of spreads and slides were transferred to two satellite scoring stations for manual analysis. The use of multiple scoring stations expedited the analysis (Fig. 2).

There have been significant previous efforts to use automated metaphase finders to detect and score cytogenetic biodosimetry endpoints (Lloyd 1984; Rutovitz 1992; Blakely *et al.* 1995). In these instances, automated metaphase finders were used alone. In this work, a new concept of digital transfer of data and slides to multiple satellite scoring stations for analysis emerged and was used successfully to facilitate data acquisition (Prasanna *et al.* 1998). This concept is outlined in Figure 2. A satellite scoring station consists of a microscope with a vernier stage and a computer with Metafind satellite scoring software. Analysis at the satellite scoring station involves recalling the originally detected spreads by a metaphase finder in another microscope station and using the computer-assisted scoring sheets in the remote station. In this approach, a single metaphase finder can support simultaneous scoring at multiple stations by different investigators; this results in saved time and an increase in effective throughput.

**Lymphocyte-dicentric calibration curves.** Since the introduction by Bender and Gooch (Bender and Gooch 1966), the lymphocyte-dicentric assay has been the generally accepted

method for biodosimetric dose assessment in cases of accidental and occupational overexposures. This approach is based on the use of *in vitro*-generated calibration curves for various radiation qualities. Experiments were performed at AFRRI to produce lymphocyte-dicentric calibration curves using an established protocol (I.A.E.A. 2001). The number of cells scored, the mean, and the frequency distribution of dicentrics per cell are presented for  $^{60}\text{Co}$  gamma rays, 250-kVp x rays, and fission neutrons and are shown in Tables 2–4. Progressive increases in radiation doses result in decreases in the fraction of cells with no dicentrics and increases in the fraction with dicentrics. These dose-response data for dicentric yields, with the one exception of  $^{60}\text{Co}$  gamma rays at a dose of 2 Gy, fit a Poisson distribution as determined by the  $\sigma^2/y$  and Papworth test (Papworth 1970). These findings of Poisson statistics are consistent with published findings from similar experiments by others (Edwards *et al.* 1979).

The classical hypothesis of aberration induction is used for the quantitative derivation of dose-effect relationships. In this model, two lesions are required for producing a dicentric, and these lesions may arise from one or two independent ionizing tracks. Dicentrics produced by single track events are proportional to the dose of radiation ( $\alpha D$ ), while the yield of dicentrics induced by two separate track events are proportional to the square of the dose ( $\beta D^2$ ). Following exposure of lymphocytes to low-LET radiation, such as 250-kVp x rays or  $^{60}\text{Co}$  gamma rays, the dicentric yield ( $Y$ ) has been shown to best fit to a linear quadratic model.

Dose responses for the mean number of dicentrics per cell for the three radiation sources are shown in Figure 4. The data at these two photon energies are consistent with the LET dependen-

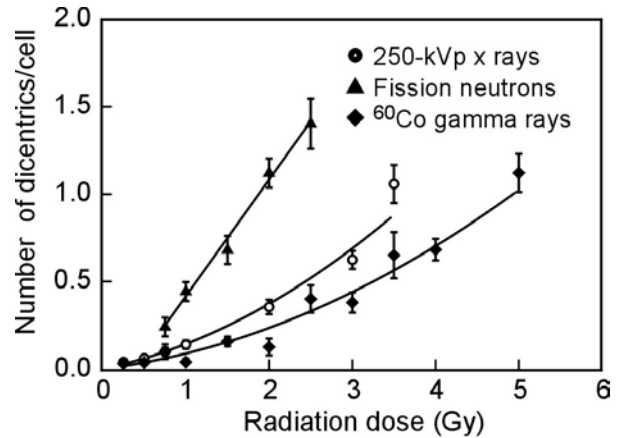


**Figure 4.** Dose-response calibration curves for the induction of dicentrics in human lymphocytes following *in vitro* exposure to  $^{60}\text{Co}$  gamma rays, 250-kVp x rays, and fission neutrons. The mean number of dicentrics per cell as a function of radiation dose was fitted to a linear-quadratic equation  $Y = \alpha D + \beta D^2$  for low-LET radiation, 250-kVp x rays, and  $^{60}\text{Co}$  gamma rays; for fission-neutrons the yield was fitted to a straight line ( $Y = \alpha D$ ) by the weighted least squares regression method. Weights were based on the reciprocal of the SE of the mean squared. These results represent the pooled mean from  $\geq 3$  independent experiments. Error bars represent SE of the mean.

cy for dicentric yields as described for low-LET sources spanning a broad range of energy (Straume 1995). Fitted data for low-LET radiation sources were  $(0.098 \pm 0.0209) D + (0.044 \pm 0.0093) D^2$  for  $^{60}\text{Co}$  gamma rays  $r = 0.999$  and  $(0.059 \pm 0.0136) D + (0.029 \pm 0.0046) D^2$  for x rays  $r = 0.995$ . These findings are in good general agreement with published findings of others. For example, AFRRI's dicentric  $^{60}\text{Co}$  gamma-ray (Fig. 5A) and x-ray (Fig. 5B) dose-response data are compared with similar published studies from other laboratories (Edwards 1997; Lloyd *et al.* 1987; Bauchinger *et al.* 1984; Bauchinger *et al.* 1979; N.C.R.P. 1990; Schmid *et al.* 1984).

## Dose Response Relationships for Dicentric Yield

**Table 2.** Distribution of dicentrics in human lymphocytes exposed *in vitro* to  $^{60}\text{Co}$  gamma rays.\*

Dose (Gy)	Number of metaphases	Frequency of dicentrics					Total/meta-phase $\pm$ SE	$\sigma^2/\mu$ , ratio $\pm$ SE	
		0	1	2	3	4			
0	395	1.00	-	-	-	-	-	-	-
0.25	332	0.9698	0.0301	-	-	-	0.0301 $\pm$ 0.0094	0.97 $\pm$ 0.08	-0.37
0.50	329	0.9640	0.0365	-	-	-	0.0365 $\pm$ 0.0104	0.97 $\pm$ 0.08	-0.45
0.75	51	0.9020	0.0980	-	-	-	0.0980 $\pm$ 0.0421	0.92 $\pm$ 0.20	-0.45
1.0	103	0.9610	0.0390	-	-	-	0.0390 $\pm$ 0.0190	0.97 $\pm$ 0.14	-0.24
1.5	191	0.8482	0.1466	0.0052	-	-	0.1570 $\pm$ 0.0274	0.91 $\pm$ 0.10	-0.85
2.0	80	0.9125	0.0500	0.0375	-	-	0.1250 $\pm$ 0.0483	1.49 $\pm$ 0.16	3.27
2.5	65	0.6615	0.2923	0.0308	0.0154	-	0.4001 $\pm$ 0.0785	1.00 $\pm$ 0.18	0.00
3.0	108	0.6852	0.2500	0.0648	-	-	0.3796 $\pm$ 0.0584	0.97 $\pm$ 0.14	-0.22
3.5	40	0.5250	0.3500	0.0750	0.0500	-	0.6500 $\pm$ 0.1318	1.07 $\pm$ 0.23	0.31
4.0	173	0.4913	0.3757	0.0983	0.0289	0.0058	0.6822 $\pm$ 0.0618	0.97 $\pm$ 0.14	-0.30
5.0	91	0.2967	0.4286	0.1758	0.0550	0.0440	1.1208 $\pm$ 0.1092	0.97 $\pm$ 0.15	-0.21

**Table 3.** Distribution of dicentrics in human lymphocytes exposed *in vitro* to 250 kVp x rays.\*

Dose (Gy)	Number of metaphases	Frequency of dicentrics					Total/meta-phase $\pm$ SE	$\sigma^2/\mu$ , ratio $\pm$ SE	
		0	1	2	3	5			
0	395	1.00	-	-	-	-	-	-	-
0.25	235	0.9617	0.0383	-	-	-	0.0383 $\pm$ 0.0125	0.97 $\pm$ 0.09	-0.39
0.50	185	0.9405	0.0595	-	-	-	0.0595 $\pm$ 0.0174	0.95 $\pm$ 0.10	-0.55
0.75	153	0.9020	0.0980	-	-	-	0.0980 $\pm$ 0.0240	0.91 $\pm$ 0.11	-0.83
1.0	216	0.8657	0.1296	0.0046	-	-	0.1388 $\pm$ 0.0245	0.93 $\pm$ 0.10	-0.72
2.0	201	0.6970	0.254	0.0500	-	-	0.3540 $\pm$ 0.0410	0.93 $\pm$ 0.10	-0.67
3.0	202	0.5149	0.3614	0.1089	0.0149	-	0.6239 $\pm$ 0.0519	0.87 $\pm$ 0.10	-1.28
3.5	87	0.3448	0.3563	0.2184	0.0690	0.0115	1.0575 $\pm$ 0.1089	0.98 $\pm$ 0.15	-0.16

**Table 4.** Distribution of dicentrics in human lymphocytes exposed *in vitro* to fission neutrons.\*

Dose (Gy)	Number of metaphases	Frequency of dicentrics					Total/meta-phase $\pm$ SE	$\sigma^2/\mu$ , ratio $\pm$ SE	
		0	1	2	3	4			
0	395	1.00	-	-	-	-	-	-	-
0.75	100	0.8100	0.1400	0.0500	-	-	0.2400 $\pm$ 0.0534	1.19 $\pm$ 0.14	1.36
1.0	138	0.6377	0.2826	0.0797	-	-	0.4420 $\pm$ 0.0544	0.93 $\pm$ 0.12	-0.62
1.5	100	0.5000	0.3500	0.1200	0.0300	-	0.6800 $\pm$ 0.0803	0.95 $\pm$ 0.14	-0.37
2.0	149	0.3154	0.3624	0.2349	0.0604	0.0269	1.1210 $\pm$ 0.0830	0.92 $\pm$ 0.12	-0.73
2.5	72	0.2778	0.3056	0.2222	0.1250	0.0694	1.4026 $\pm$ 0.1435	1.06 $\pm$ 0.17	0.34

\*Note: Distribution analysis of the number of dicentrics was analyzed as described by Papworth (Papworth 1970) using  $\sigma^2/\mu$  and the overdispersion parameter ( $\mu$ ). A  $\mu$  value between -1.96 and 1.96 indicates a Poisson distribution.

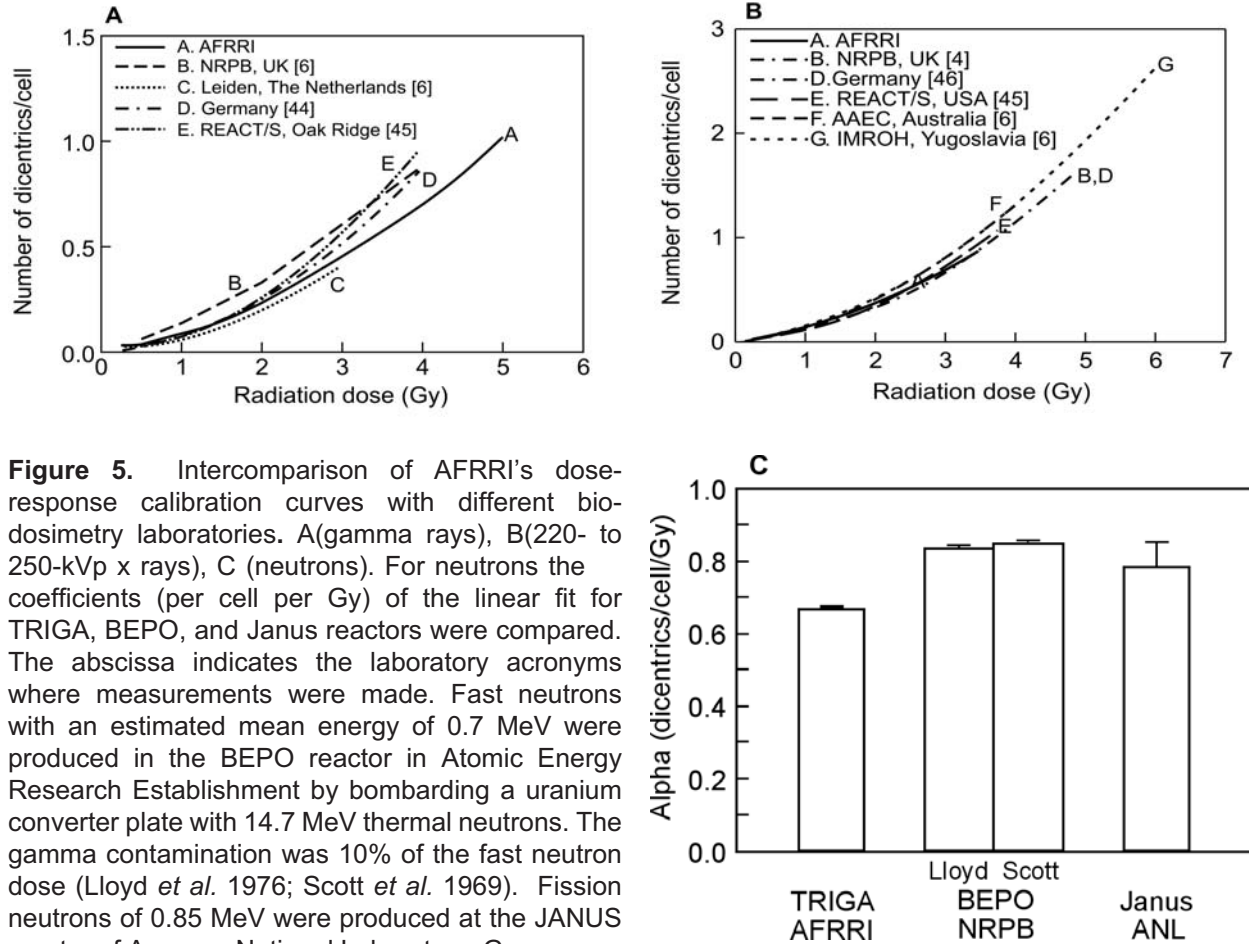


**Figure 5.** Intercomparison of AFRRI's dose-response calibration curves with different biodosimetry laboratories. A(gamma rays), B(220- to 250-kVp x rays), C (neutrons). For neutrons the coefficients (per cell per Gy) of the linear fit for TRIGA, BEPO, and Janus reactors were compared. The abscissa indicates the laboratory acronyms where measurements were made. Fast neutrons with an estimated mean energy of 0.7 MeV were produced in the BEPO reactor in Atomic Energy Research Establishment by bombarding a uranium converter plate with 14.7 MeV thermal neutrons. The gamma contamination was 10% of the fast neutron dose (Lloyd *et al.* 1976; Scott *et al.* 1969). Fission neutrons of 0.85 MeV were produced at the JANUS reactor of Argonne National Laboratory. Gamma ray contribution was approximately 3% of the neutron dose.

However, significant differences exist between laboratories. Inter-laboratory variations in dose-response curves, aberration yields, and dose estimates for simulated accidents were noted by Lloyd *et al.* (Lloyd *et al.* 1987) in a collaborative biodosimetry exercise conducted with the support of International Atomic Energy Agency (IAEA). Discrepancies related to dose-response curves and aberration yields may be overcome by adopting centromere painting with a pan-centromeric DNA-hybridization probe for aberration analysis (Kolanko *et al.* 1993; Schmid *et al.* 1995; Roy *et al.* 1996). We are currently studying the influence of centromere painting on the detection of dicentrics. In order to avoid uncertainty in dose assessment, it is advised that each laboratory use its own calibration curve rather than using calibration curves produced by

another laboratory (I.A.E.A. 2001). The formation of dicentric aberrations by high-LET irradiation are dominated by single-track events, hence their yield is proportional to the dose of radiation ( $\alpha D$ ). Dose-response relationships for dicentric yields following exposure to AFRRI fission neutrons were fitted with the mathematical function  $Y = \alpha D$  over a dose range from 0.75 to 2.5 Gy. The  $\alpha$  coefficient was  $0.677 \pm 0.0003$  ( $r = 0.996$ ). This finding is comparable to similar studies performed at  $^{235}\text{U}$ -reactor fission-neutron facilities (Lloyd *et al.* 1976; Scott *et al.* 1969; Carrano 1975) (Fig. 5C). These data are also consistent with the LET dependency seen for dicentric yields as described for particle sources spanning a broad range of energy (Edwards 1997).

Irradiation of blood lymphocytes *in vitro* or *in vivo* produces similar levels of dicentrics per

cGy (I.A.E.A.2001). Therefore, observed yields of dicentrics in an exposed person's blood lymphocytes may be used to assess previous radiation exposure by comparison with an *in vitro*-produced dose-response calibration curve. The influence of sample size on the uncertainties on the estimated dose is discussed in the appendix. Chromosome aberration analysis remains a valuable radiation dose assessment method for biological dosimetry in accidental and occupational radiation exposures.

### **Acknowledgements**

The Armed Forces Radiobiology Research Institute, under work unit AFRRI-98-3 and cooperative research and development agreement (CRADA) AFRRI/LAI-95 supported this research. A.W. Khusein was supported by a fel-

lowship from the International Atomic Energy Agency, Vienna. The views expressed are those of the authors; no endorsement by AFRRI has been given or inferred. The expert contributions of the Radiation Sciences Department staff members, who provided technical assistance in repeated radiation exposures and dosimetry support, is gratefully acknowledged. The expert assistance of T.D. Roberge, S.M. Gribben, M.D. Pyle, and J. Sanders is appreciated. The editorial assistance of M. Greenville and E. Pirrung, and desktop design layout by A. Ward are also greatly appreciated. We also wish to thank, for their assistance and helpful discussions, E.E. Kearsley, Ph.D. (NCRP, Bethesda, MD), K.S. Kumar, Ph.D. (AFRRI, Bethesda, MD), L. Gayle Littlefield, Ph.D. (ORISE, Oak Ridge, TN), and A.T. Natarajan, Ph.D. (Leiden University, The Netherlands).

## Appendix

Estimation of Radiation Dose: Influence of Sample Size on Uncertainties. Radiation dose is estimated without any difficulty by comparing the measured yield of dicentric chromosomes in an exposed individual's blood lymphocytes with an *in-vitro*-generated calibration curve. However, there is no unified way of deriving the uncertainty on the estimated dose, which is normally expressed as a confidence interval. By convention, a 95% confidence limit is chosen as the standard, meaning that the estimated dose is accurate 95 out of 100 times. The uncertainty on the estimated dose arises from uncertainties associated with two factors: (1) the Poisson nature of the yield of dicentric chromosomes and (2) the calibration curve. The nature of the distribution of dicentric chromosomes after exposure to different radiation qualities is shown in Tables 2-4.

An example of increasing the number of metaphases analyzed from 50 to 500 for varying number of dicentric chromosomes observed on the 95% confidence limits for estimated radiation doses between 0.08 and 4.93 Gy is shown (Table A1). These estimations were derived from the coefficients of our calibration curve for gamma radiation. Generally, analysis of 200 metaphases is sufficient to estimate a dose with reasonable confidence in accidental exposure levels of military relevance.

The 95% confidence limits for our calibration curves for different radiation qualities are shown in Figure A1. The coefficients of these calibration curves are used to determine radiation doses in accidental exposures of military personnel.

**Table A1.** An example of the effect of the sample size on lower and upper 95% confidence limits on the estimated whole-body equivalent after acute exposure using the AFRRI <sup>60</sup>Co gamma-ray calibration curve.

Number of dicentric chromosomes per cell	Mean dose (cGy)	Lower confidence limit (cGy)			Upper confidence limit (cGy)		
		Sample size			Sample size		
		50	200	500	50	200	500
0.005	8	< 2	< 2	< 2	118	58	39
0.010	16	< 2	< 2	4	126	69	52
0.025	36	< 2	9	14	148	95	78
0.050	64	9	25	33	176	126	110
0.100	110	33	59	70	221	172	157
0.250	209	119	150	163	329	273	254
0.500	325	227	265	278	454	401	381
0.750	416	316	348	362	566	504	488
1.000	493	383	417	431	655	598	581

## Dose Response Relationships for Dicentric Yield

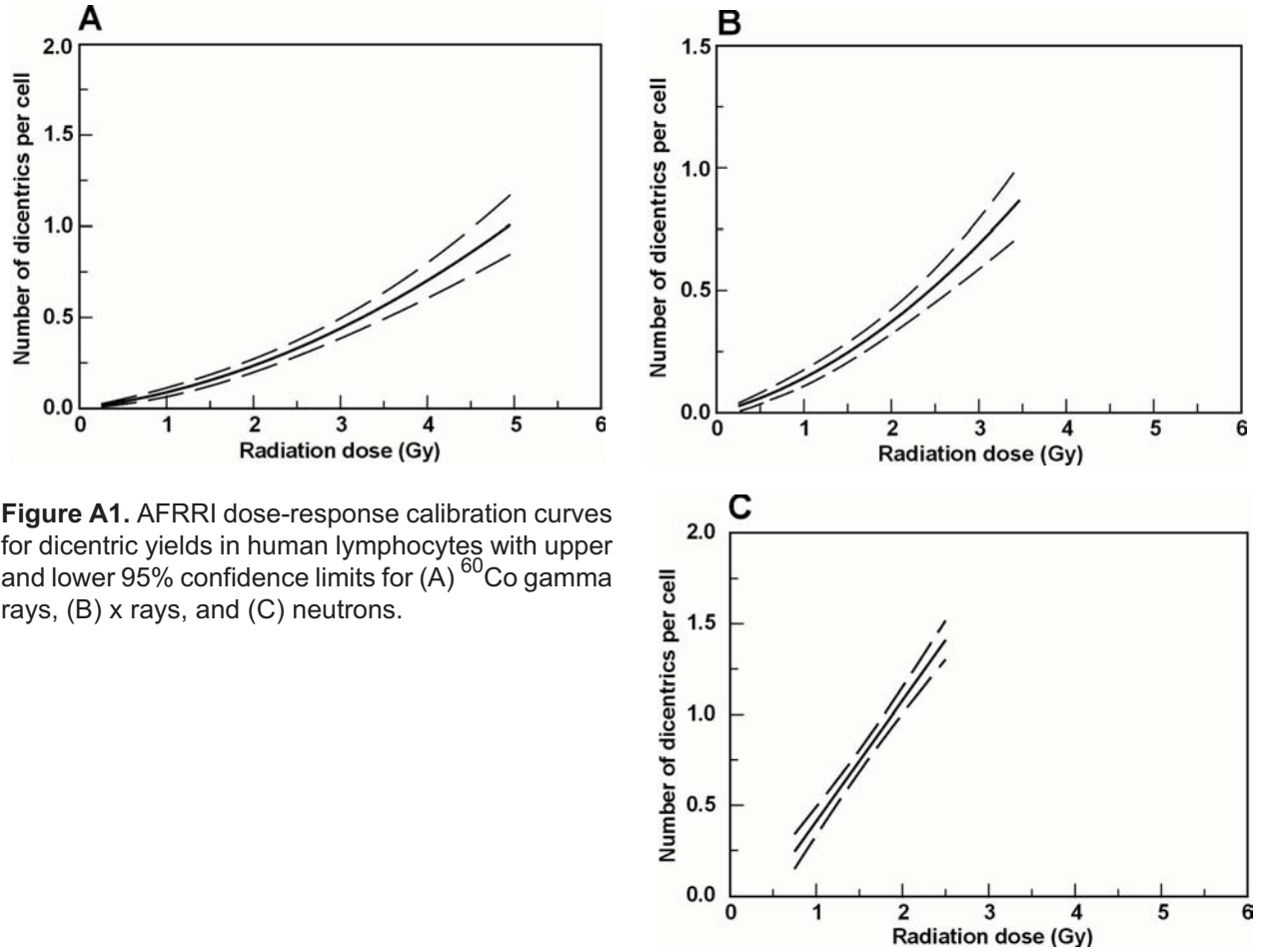


**Figure A1.** AFRRRI dose-response calibration curves for dicentric yields in human lymphocytes with upper and lower 95% confidence limits for (A)  $^{60}\text{Co}$  gamma rays, (B) x rays, and (C) neutrons.

## References

---

- A.A.P.M. (American Association of Physicists in Medicine), Radiation Therapy Committee Task Group 21 (1983) A protocol for determination of absorbed dose from high-energy photon and electron beams. *Medical Physics*, 10:741-747.
- Attix FH (1986) *Introduction to Radiological Physics and Radiation Dosimetry*. New York: John Wiley & Sons.
- Bauchinger M (1983) Microdosimetric aspects of the induction of chromosome aberrations. In: Ishihara T, Sasaki MS (eds) *Radiation Induced Chromosome Damage in Man*. New York: Alan R. Liss, Inc., 1-22.
- Bauchinger M, Koester L, Schmid E, Dresch J, Streng S (1984) Chromosome aberrations in human lymphocytes induced by neutrons. *International Journal of Radiation Biology*, 45:449-457.
- Bauchinger M, Schmid E, Dresch J (1979) Calculation of the dose-rate dependence of the dicentric yield after Co  $\gamma$ -irradiation of human lymphocytes. *International Journal of Radiation Biology*, 35:229-233.
- Bender MA, Gooch PC (1966) Somatic chromosome aberrations induced by human whole-body irradiation: The "Recuplex" criticality accident. *Radiation Research*, 29:568-582.
- Biavati MH, Boer E (1996) D(Y) spectragamma rays. In: *Annual Report on Research Project*. New York: Radiological Research Laboratory, Columbia University, 87-101.
- Blakely WF, Benevides LA, Gerstenberg HM (1995) Fission-neutron effects on chromosome damage in Chinese hamster V79 cells: Use of the daughter-and granddaughter- microcolony micronuclei assay. In: Hagan U, Jung H, Strefler C (eds) *Radiation Research 1895-1995, Congress Proceedings, Vol. 2: Congress Lectures*. Wurzburg, Germany: 10<sup>th</sup> ICRR Society, 344-347.
- Blakely WF, Prasanna PGS, Kolanko CJ, Pyle MD, Mosbrook DM, Loats AS, Rippeon TL, Loats H (1995) Application of premature chromosome condensation assay in simulated partial-body radiation exposures: Evaluation of the use of an automated metaphase finder. *Stem Cells*, 13:223-230.
- Carrano AV (1975) Induction of chromosomal aberrations human lymphocytes by x rays and fission neutrons: Dependence on cell cycle stage. *Radiation Research*, 63:403-421.
- Carter RE, Verrelli DM (1973) AFRRRI Cobalt Whole-body Irradiator (AFRRRI Technical Report 73-3). Bethesda, MD: Armed Forces Radiobiology Research Institute, 1-8.
- Edwards AA (1997) The use of chromosomal aberrations in human lymphocytes for biological dosimetry. *Radiation Research*, 148:S39-S44.
- Edwards AA, Lloyd DC, Purrott RJ (1979) Radiation induced chromosome aberrations and the Poisson distribution. *Radiation and Environmental Biophysics*, 16:89-100.
- Eisenhauer C (1991) AFRRRI Neutron Spectrum Directory. Gaithersburg, MD: National Institute of Standards and Technology, 1-58.
- Fisher DR, Harty R (1982) The microdosimetry of lymphocytes irradiated by alpha particles. *International Journal of Radiation Biology*. 41: 315-324.
- Gerstenberg, H.M. (1989) Application of microdosimetry to battlefield neutron spectra. In: *Proceedings of the 1989 Workshop of the RSG-5 Physical Dosimetry Subcommittee*. Arcueil, France: ETCA.
- Gerstenberg HM (1991) Comparison of Y spectra from the TRIGA and Janus reactors: The implication for dose rate studies. In: Chapman JD, Dewey WC, Whitmore GF (eds) *Radiation*

## Dose Response Relationships for Dicentric Yield

Research: A Twentieth Century Perspective, Vol. 1: Congress Abstracts. San Diego: Academic Press Inc., 110.

Greenstock CL, Trivedi A (1994) Biological and biophysical techniques to assess radiation exposure: A perspective. *Progress in Biophysics and Molecular Biology*, 61:81-130.

I.A.E.A. (2001) Cytogenetic Analysis for Radiation Dose Assessment: A Manual. (Technical Report 405). Vienna: International Atomic Energy Agency.

I.C.R.U. (1973) Measurement of Absorbed Dose in a Phantom Irradiated by a Single Beam of X or Gamma Rays (Report 23). Washington DC International Commission on Radiation Units and Measurements.

I.C.R.U. (1977) Neutron Dosimetry for Biology and Medicine (Report 26). Bethesda, MD: International Commission on Radiation Units and Measurements.

I.C.R.U. (1980) Linear Energy Transfer (Report 16). Washington DC: International Commission on Radiological Units.

I.C.R.U. (1993) Quantities and Units in Radiation Protection Dosimetry (Report 51). Bethesda, MD: International Commission on Radiological Units.

Keifer J (1990) Biological Radiation Effects. New York: Springer-Verlag, 444.

Kolanko CJ, Prasanna PGS, Nath J, Blakely WF (1993) PCR synthesis of a human pancentromeric DNA hybridization probe and detection of *in situ* probe hybridization using color pigment/immunostaining. In: Proceedings of NATO Workshop on Biomedical Aspects of Nuclear Defense, Panel 8, Research Study Group 23 on Ionizing Radiation. Bethesda, MD.

Lloyd DC (1984) An overview of radiation dosimetry by conventional cytogenetic methods. In: Eisert WG, Medelsohn ML (eds) Biological

Dosimetry: Cytogenetic Approaches to Mammalian Systems. New York: Springer and Verlag, 3-14.

Lloyd DC, Edwards AA, Prosser JS, Barjaktarovic N, Brown JK, Horvat D, Ismail SR, Koteles GJ, Almassy Z, Krepinsky A, Kucerova M, Littlefield LG, Mukherjee U, Natarajan AT, Sasaki MS (1987) A collaborative exercise on cytogenetic dosimetry for simulated whole and partial body accidental irradiation. *Mutation Research*, 179:197-208.

Lloyd DC, Purrott RJ, Dolphin GW, Edwards AA (1976) Chromosome aberrations induced in human lymphocytes by neutron irradiation. *International Journal of Radiation Biology*, 29: 169-82.

Marshall IR, Williamson FS (1985) Microdosimetric measurements of Janus neutrons. *Radiation Protection Dosimetry*, 13:111-115.

Muller WU, Streffer C (1991) Biological indicators of radiation damage. *International Journal of Radiation Biology*, 59:863-873.

N.C.R.P. (1990) The Relative Biological Effectiveness of Radiations of Different Quality (Report 104). Bethesda, MD: Recommendations of the National Council on Radiation Protection and Measurements, National Radiological Protection Board, 28-48.

N.I.S.T. (1991) Annual Progress Report in Support of Neutron Dosimetry. Gaithersburg, MD: National Institute of Standards and Technology.

Papworth DG (1970) Appendix. In: Savage JRK, Sites of radiation induced chromosome exchanges. *Current Topics in Radiation*, 6: 129-194.

Prasanna PGS, Garner DC, Khusein AW, Loats H, Shehata CW, Gerstenberg HM, Blakely WF (1998) Chromosome aberration analysis for

- biological dosimetry: A real case scenario of diagnostic service supporting the U.S. armed forces. In: Proceedings of the 1996 Workshop of the Research Study Group on the Biomedical Aspects of Nuclear Defense, Panel 8, Research Study Group 23 on Ionizing Radiation. Ottawa, Canada, 5.1-5.10.
- Prasanna PGS, Kolanko CJ, Gerstenberg HM, Blakely WF (1997) Premature chromosome condensation assay for biodosimetry: Studies with fission neutrons. *Health Physics*, 72: 594-600.
- Preist JH (1977) *Medical Cytogenetics and Cell Culture*. Philadelphia: Lea and Febiger.
- Redpath JL, Antoniono RJ, Sun C, Gerstenberg HM, Blakely WF (1995) Late mitosis/early G1 phase and mid-G1 phase are not hypersensitive cell cycle phases for neoplastic transformation of HeLa x skin fibroblast human hybrid cells induced by fission-spectrum neutrons. *Radiation Research*, 141:37-43.
- Rossi HH (1959) Specification of radiation quality. *Radiation Research*, 10:522-531.
- Roy L, Sorokine-Durm I, Voisin P (1996) Comparison between fluorescence *in situ* hybridization and conventional cytogenetics for dicentric scoring: A first-step validation for the use of FISH in biological dosimetry. *International Journal of Radiation Biology*, 70:665-669.
- Rutovitz D (1992) Reflections on the past, present and future of automated aberration scoring systems for radiation dosimetry. *Journal of Radiation Research*, 33 (Supplement):1-30.
- Schmid E, Bauchinger M, Steng S, Nahrstedt U (1984) The effect of 220-kVp x rays with different spectra on the dose response of chromosome aberrations in human lymphocytes. *Radiation Environmental Biophysics*, 23: 305-309.
- Schmid E, Braselmann H, Nahrstedt U (1995) Comparison of  $\gamma$ -ray induced dicentric yields in human lymphocytes measured by conventional analysis and FISH. *Mutation Research*, 348: 125-130.
- Scott D, Sharpe H, Batchelor AL, Evans HJ, Papworth DG (1969) Radiation-induced chromosome damage in human peripheral blood lymphocytes *in vitro* 1. RBE and dose-rate studies with fission neutrons. *Mutation Research*, 8:367-381.
- Stankus AA, Xapsos MA, Kolanko CJ, Gerstenberg HM, Blakely WF (1995) Energy deposition events produced by fission neutrons in aqueous solutions of plasmid DNA. *International Journal of Radiation Biology*, 68:1-9.
- Straume T (1995) High energy gamma rays in Hiroshima and Nagasaki: Implications for risk and WR. *Health Physics*, 69:954-956.
- Turner JE (1992) An introduction to microdosimetry. *Radiation Protection Management*, 9:25-58.
- Verbinski VV, Cassapakis CG, Hagan WK, Ferlic K, Daxon E (1981) Calculation of the Neutron and Gamma-ray Environment in and around the AFRRI TRIGA Reactor (DNA 5793F-2). Washington, DC: Defense Nuclear Agency, 1-262.
- Watt DE, Alkharam AS, Child MB, Salikin MS (1994) Dose as a damage specifier in radiobiology for radiation protection. *Radiation Research*, 139:249-251.
- Zeman GH, Ferlic KP (1984) Paired ion chamber constants for fission gamma-neutron fields (Technical Report). Bethesda, MD: Armed Forces Radiobiology Research Institute, 84-8.

## Dose Response Relationships for Dicentric Yield

## Distribution List

### **DEPARTMENT OF DEFENSE**

ARMED FORCES RADIOBIOLOGY RESEARCH INSTITUTE  
ATTN: INFORMATION SERVICES DIVISION  
ATTN: TECHNICAL LIBRARY

ARMY/AIR FORCE JOINT MEDICAL LIBRARY  
ATTN: DASG-AAFJML

ASSISTANT TO THE SECRETARY OF DEFENSE  
ATTN: AE  
ATTN: HA(IA)

DEFENSE SPECIAL WEAPONS AGENCY  
ATTN: TITL  
ATTN: DDIR  
ATTN: RAEM  
ATTN: MID

DEFENSE TECHNICAL INFORMATION CENTER  
ATTN: ACQUISITION  
ATTN: ADMINISTRATOR

ALBUQUERQUE OPERATION, DEFENSE THREAT  
REDUCTION AGENCY  
ATTN: DASIAC  
ATTN: AORSE

INTERSERVICE NUCLEAR WEAPONS SCHOOL  
ATTN: DIRECTOR

LAWRENCE LIVERMORE NATIONAL LABORATORY  
ATTN: LIBRARY

UNDER SECRETARY OF DEFENSE (ACQUISITION)  
ATTN: OUSD(A)/R&E

UNIFORMED SERVICES UNIVERSITY  
ATTN: LIBRARY

### **DEPARTMENT OF THE ARMY**

HARRY DIAMOND LABORATORIES  
ATTN: SLCSM-SE

OFFICE OF THE SURGEON GENERAL  
ATTN: MEDDH-N

U.S. ARMY AEROMEDICAL RESEARCH LABORATORY  
ATTN: SCIENCE SUPPORT CENTER

U.S. ARMY CHEMICAL RESEARCH, DEVELOPMENT, &  
ENGINEERING CENTER  
ATTN: SMCCR-RST

U.S. ARMY INSTITUTE OF SURGICAL RESEARCH  
ATTN: COMMANDER

U.S. ARMY MEDICAL DEPARTMENT CENTER AND SCHOOL  
ATTN: MCCS-FCM

U.S. ARMY MEDICAL RESEARCH AND MATERIEL COMMAND  
ATTN: COMMANDER

U.S. ARMY MEDICAL RESEARCH INSTITUTE OF CHEMICAL  
DEFENSE

ATTN: MCMR-UV-R

U.S. ARMY NUCLEAR AND CHEMICAL AGENCY  
ATTN: MONA-NU

U.S. ARMY RESEARCH INSTITUTE OF ENVIRONMENTAL  
MEDICINE

ATTN: DIRECTOR OF RESEARCH

U.S. ARMY RESEARCH LABORATORY  
ATTN: DIRECTOR

WALTER REED ARMY INSTITUTE OF RESEARCH  
ATTN: DIVISION OF EXPERIMENTAL  
THERAPEUTICS

### **DEPARTMENT OF THE NAVY**

BUREAU OF MEDICINE & SURGERY  
ATTN: CHIEF

NAVAL AEROSPACE MEDICAL RESEARCH LABORATORY  
ATTN: COMMANDING OFFICER

NAVAL MEDICAL RESEARCH AND DEVELOPMENT  
COMMAND  
ATTN: CODE 42

NAVAL MEDICAL RESEARCH INSTITUTE  
ATTN: LIBRARY

NAVAL RESEARCH LABORATORY  
ATTN: LIBRARY

OFFICE OF NAVAL RESEARCH  
ATTN: BIOLOGICAL & BIOMEDICAL S&T

### **DEPARTMENT OF THE AIR FORCE**

BROOKS AIR FORCE BASE  
ATTN: AL/OEBZ

OFFICE OF AEROSPACE STUDIES  
ATTN: OAS/XRS

OFFICE OF THE SURGEON GENERAL  
ATTN: HQ AFMOA/SGPT  
ATTN: HQ USAF/SGES

U.S. AIR FORCE ACADEMY  
ATTN: HQ USAFA/DFBL

U.S. AIR FORCE OFFICE OF SCIENTIFIC RESEARCH  
ATTN: DIRECTOR OF CHEMISTRY & LIFE  
SCIENCES

**OTHER FEDERAL GOVERNMENT**

ARGONNE NATIONAL LABORATORY  
ATTN: ACQUISITIONS

BROOKHAVEN NATIONAL LABORATORY  
ATTN: RESEARCH LIBRARY, REPORTS SECTION

CENTER FOR DEVICES AND RADIOLOGICAL HEALTH  
ATTN: DIRECTOR

GOVERNMENT PRINTING OFFICE  
ATTN: DEPOSITORY ADMINISTRATION BRANCH  
ATTN: CONSIGNED BRANCH

LIBRARY OF CONGRESS  
ATTN: UNIT X

LOS ALAMOS NATIONAL LABORATORY  
ATTN: REPORT LIBRARY

NATIONAL AERONAUTICS AND SPACE ADMINISTRATION  
ATTN: RADLAB

NATIONAL AERONAUTICS AND SPACE ADMINISTRATION  
GODDARD SPACE FLIGHT CENTER  
ATTN: LIBRARY

NATIONAL CANCER INSTITUTE  
ATTN: RADIATION RESEARCH PROGRAM

U.S. DEPARTMENT OF ENERGY  
ATTN: LIBRARY

U.S. FOOD AND DRUG ADMINISTRATION  
ATTN: WINCHESTER ENGINEERING AND  
ANALYTICAL CENTER

U.S. NUCLEAR REGULATORY COMMISSION  
ATTN: LIBRARY

**RESEARCH AND OTHER ORGANIZATIONS**

AUSTRALIAN DEFENCE FORCE  
ATTN: SURGEON GENERAL

AUTRE, INC.  
ATTN: PRESIDENT

BRITISH LIBRARY

ATTN: ACQUISITIONS UNIT

CENTRE DE RECHERCHES DU SERVICE DE SANTE DES  
ARMEES  
ATTN: DIRECTOR

FEDERAL ARMED FORCES DEFENSE SCIENCE AGENCY FOR  
NBC PROTECTION  
ATTN: LIBRARY

FOA NBC DEFENCE  
ATTN: LIBRARY

INHALATION TOXICOLOGY RESEARCH INSTITUTE  
ATTN: LIBRARY

INSTITUTE OF NUCLEAR MEDICINE AND ALLIED SCIENCES  
ATTN: DIRECTOR

INSTITUTE OF RADIOBIOLOGY, ARMED FORCES MEDICAL  
ACADEMY  
ATTN: DIRECTOR

OAK RIDGE ASSOCIATED UNIVERSITIES  
ATTN: MEDICAL LIBRARY

RESEARCH CENTER OF SPACECRAFT RADIATION SAFETY  
ATTN: DIRECTOR

RUTGERS UNIVERSITY  
ATTN: LIBRARY OF SCIENCE AND MEDICINE

UNIVERSITY OF CALIFORNIA  
ATTN: DIRECTOR, INSTITUTE OF TOXICOLOGY  
& ENVIRONMENTAL HEALTH  
ATTN: LIBRARY, LAWRENCE BERKELEY  
LABORATORY

UNIVERSITY OF CINCINNATI  
ATTN: UNIVERSITY HOSPITAL, RADIOISOTOPE  
LABORATORY

XAVIER UNIVERSITY OF LOUISIANA  
ATTN: COLLEGE OF PHARMACY

AUTORIDAD REGULATORIA NUCLEAR  
CENTRO DE INFORMACION

**REPORT DOCUMENTATION PAGE**

*Form Approved*  
*OMB No. 0704-0188*

Public reporting burden for this collection of information is estimated to average 1 hour per response, including the time for reviewing instructions, searching existing data sources gathering and maintaining the data needed, and completing and reviewing the collection of information. Send comments regarding this burden estimate or any other aspect of this collection of information, including suggestions for reducing the burden, to Washington Headquarters Services, Directorate for Information Operations and Reports, 1215 Jefferson Davis Highway, Suite 1204, Arlington, VA 22202-4302, and to the Office of Management and Budget, Paperwork Reduction Project (0704-0188), Washington, DC 20503.

1. AGENCY USE ONLY (Leave blank)		2. REPORT DATE May 2002		3. REPORT TYPE AND DATES COVERED Special Publication	
4. TITLE AND SUBTITLE AFRRI's Gamma-Ray, X-Ray, and Fission-Neutron Calibration Curves for the Lymphocyte Dicentric Assay: Application of a Metaphase Finder System				5. FUNDING NUMBERS	
6. AUTHOR(S) Prasanna PGS, Loats H, Gerstenberg HM, Torres BN, Shehata CW, Duffy KL, Floura RS, Khusen AW, Jackson WE, Blakely WF					
7. PERFORMING ORGANIZATION NAME(S) AND ADDRESS(ES) Armed Forces Radiobiology Research Institute 8901 Wisconsin Avenue Bethesda, MD 20889-5603				8. PERFORMING ORGANIZATION REPORT NUMBER	
9. SPONSORING/MONITORING AGENCY NAME(S) AND ADDRESS(ES)				10. SPONSORING/MONITORING AGENCY REPORT NUMBER	
11. SUPPLEMENTARY NOTES					
12 a. DISTRIBUTION/AVAILABILITY STATEMENT Approved for public release; distribution unlimited.				12 b. DISTRIBUTION CODE	
13. ABSTRACT (Maximum 200 words)  Facilities are established at the Armed Forces Radiobiology Research Institute (AFRRI) to perform radiation-induced chromosome aberration analysis for biological dosimetry. Whole blood from healthy human volunteers was used after obtaining informed consent. Peripheral blood lymphocytes were exposed <i>in vitro</i> to different types of radiation; <sup>60</sup> Co gamma rays ( $E_{\gamma}=1.25$ MeV, mean of the absorbed dose distribution of the lineal energy, $y_D=1.9$ keV/ $\mu$ m, 1 Gy/min); x rays (250 kVp, $E = 83$ keV, $y_D = 4$ keV/ $\mu$ m, 1 Gy/min); or a fission-spectrum neutron source ( $E=0.71$ MeV, $y_D= 65$ keV/ $\mu$ m, 0.25 Gy/min). Distribution of radiation-induced dicentrics among cells exhibited Poisson statistics as characterized by the Papworth method (Papworth 1970). Dose-response relationships for the yield of dicentrics for photon sources were fitted with a linear-quadratic model using the maximum-likelihood method and for the neutron source by a weighted linear regression method. Comparison of the data with other published studies is presented. The dose-response relationships for dicentric induction by low- and high-linear energy transfer (LET) radiation are consistent with the single- and two-track model of aberration formation, $Y = \alpha D + \beta D^2$ . An increase in $y_D$ resulted in an increase in dicentric yield. As expected, fission neutrons induced a significantly higher yield of dicentrics than that caused by low-LET sources. The linear component of the model, corresponding to damage caused by single-tracks, is predominant with fission neutrons so that the dose-effect relationship is essentially linear. An automated metaphase finder system with a satellite scoring utility was used to improve data collection.					
14. SUBJECT TERMS				15. NUMBER OF PAGES 36	
				16. PRICE CODE	
17. SECURITY CLASSIFICATION OF REPORT UNCLASSIFIED	18. SECURITY CLASSIFICATION OF THIS PAGE UNCLASSIFIED	19. SECURITY CLASSIFICATION OF ABSTRACT UNCLASSIFIED	20. LIMITATION OF ABSTRACT UL		

SECURITY CLASSIFICATION OF THIS PAGE

CLASSIFIED BY:

DECLASSIFIED ON:

---

This publication is a product of the AFRRRI Information Services Division. Editor: Erica Pirrung. Graphic illustrators: Guy Bateman and Mark Behme. Desktop publisher: Alice Ward.

